Proceedings 10th NUMGE 2023
10th European Conference on Numerical Methods in Geotechnical Engineering
Zdravkovic L, Kontoe S, Taborda DMG, Tsiampousi A (eds)

https://doi.org/10.53243/NUMGE2023-127

Comparative numerical calculations in the context of tunnel design for nuclear waste repositories in Opalinus Clay

A. Madaschi[1] , J. Leuthold[2] , L. Cantieni[2] , L. Laloui[3]

[1]Nesol – Numerical Engineering Solutions, Lausanne, Switzerland
[2]Nagra, Wettingen, Switzerland
[3]Swiss Federal Institute of Technology in Lausanne (EPFL), Lausanne, Switzerland

ABSTRACT: The hydro-mechanical (HM) response of the host rock selected for the Swiss geological repository for radioactive waste, the Opalinus Clay (OPA), is complex, and its description requires advanced constitutive models. However, for the tunnel design, a simple design-orientated approach is envisaged. The present study uses the eADP constitutive model for numerical tunnel analyses. It considers most aspects of the OPA mechanical behaviour, such as anisotropic stiffness and strength, post-peak softening, and pre-peak anisotropic hardening. The model has been calibrated on an experimental dataset composed of 13 triaxial tests. The study focuses on the effect of softening on tunnel design aspects under project-specific conditions. It includes comparative HM FEM plane strain computations of tunnel excavations with and without post-peak softening. Displacements of the tunnel boundary and internal actions of the lining were computed for long-term conditions. The paper shows that, for high initial stresses and rock strength typical for OPA, the results obtained with a perfect plastic approach considering the residual strength are close to those obtained considering softening behaviour.

Keywords: tunnelling; anisotropy; tunnel design; nuclear-waste; finite element modelling; numerical modelling

1 INTRODUCTION

Opalinus Clay (OPA) is a claystone formation selected as the host rock for the deep geological repository of Swiss radioactive wastes for its favourable hydro-mechanical properties (Gautschi, 2017). Recently, efforts have been devoted to studying the engineering features of the rock formation and to implementing reliable modelling tools to describe the Opalinus Clay mechanical response for the repository design (Nordas et al., 2023; Nguyen et al., 2020).

In this work, an advanced constitutive model, the eADP (Madaschi et al., 2023), is used to perform a comparative numerical study on tunnel excavation for nuclear waste repositories in Opalinus Clay. This model can capture, within a robust and efficient numerical scheme, the main features of the hydro-mechanical response of OPA, namely, the strong anisotropic behaviour (transverse isotropic elasticity, strength and hardening anisotropy), the pre-peak hardening and the quasi-brittle softening response.

The model has been calibrated with an optimisation approach on an extensive database of 13 undrained triaxial tests performed by loading the samples with different angles to the material anisotropy planes. The calibrated material parameters have been used to perform a comprehensive comparative study on the tunnel excavation modelling with different parameter sets. The computations have aimed to investigate the effect of fundamental modelling assumptions on the tunnel excavation results. The focus hereby is on the impact of the anisotropic strength, anisotropic stiffness and softening behaviour since these aspects are mostly not included in less sophisticated engineering models used for structural engineering. For this purpose, a series of 2D Finite Element plane strain fully coupled hydro-mechanical simulations considering the short-and long-term behaviour of the rock have been performed.

These simulations include the computation of the Ground Response Curves (GRCs) (i.e., the tunnel convergence as a function of the support pressure) of the tunnel excavation problem for eleven support pressures from 0 to 5 Mpa, considering different parameter sets. Moreover, additional simulations have been performed to model the impact of the concrete lining on the tunnel convergence and to estimate the lining’s internal actions. The results of the comparative study enable an analysis of the sensitivity of the eADP assumptions on the rock-mass response in the short- and long-term.

2 COMPUTATIONAL MODEL

The finite element model is created in Abaqus, adopting a 2D plane strain approach with horizontal bedding planes. This assumption, together with the circular tunnel section, enables modelling one-fourth of the entire domain by exploiting the model symmetry (Figure 1).

The model layout in terms of geometry, materials, and mechanical and hydraulic boundary conditions is shown in Figure 1.

The dimensions of the model are 200 m x 200 m, and the model is divided into two parts: i. an Opalinus Clay layer 50 m thick, modelled considering the hydro-mechanical coupling adopting the eADP material model; ii. a far field rock layer 150 m thick, modelled with single phase elements and adopting an isotropic linear elastic material ($E = 5000$ MPa, $\nu = 0.3$). The layer of isotropic elastic material attenuates the effects of the boundary conditions. The radius of the tunnel is 3.1 m and corresponds to the size of an operational tunnel of the repository. The vertical and horizontal displacements are constrained at the outer boundaries, and no flow conditions are imposed on the bottom and exterior edges of the Opalinus Clay layer. The pore pressure is fixed to its initial value at the upper side of the OPA layer.

The initial stress and pore pressure fields are assumed to be constant over the entire domain. The initial effective stress state is $\sigma'_x = \sigma'_y = 13.5$ MPa, $\sigma'_z = 17.55$ MPa, and $p_w = 9$ MPa, corresponding to an overburden depth of 900 m. In these conditions, disregarding the geostatic gradient is acceptable due to the significant stress level.

The coupled hydro-mechanical problem in the Opalinus Clay layer has been solved with the classical Abaqus consolidation analysis. The hydraulic model is isotropic with a permeability of $1 \cdot 10^{-13}$ m/s (Favero et al., 2016), and a "suction cut-off" approach defines the desaturated domain around the tunnel due to excavation-induced fissures (Boldrini and Graziani, 2012).

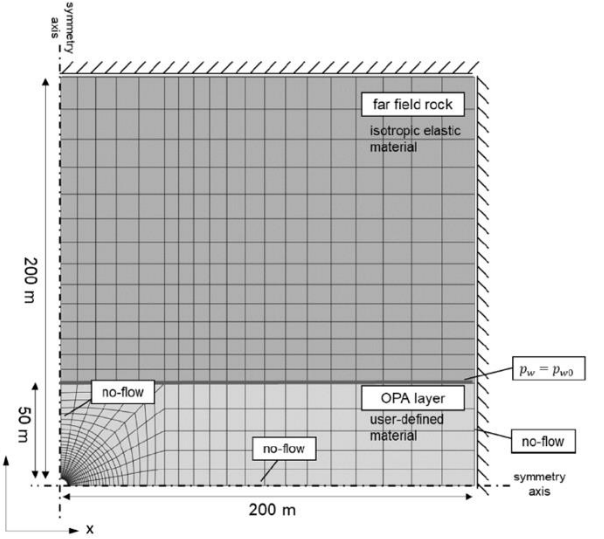

Figure 1. Geometry, mesh and boundary conditions of the 2D approach for GRC computation.

The simulations are performed in three steps:

1. Initial condition: the initial stress and pore pressure field of the corresponding overburden is imposed. Uniform pressure is applied on the tunnel surface to equilibrate the initial state.
2. Excavation – Short-term: the confining pressure applied to the tunnel surface is decreased to reach the support pressure to be analysed in undrained conditions (i.e., excavation executed in 0.1 days).
3. Long-term evolution: the drained conditions are analysed by imposing atmospheric pressure ($p_w = 0$ MPa) on the tunnel surface for 1000 years (steady state).

The domain is discretised with a structured mesh having a minimum element size at the tunnel face equal to 20 cm corresponding to 24 elements defining the excavation face. Linear 4 nodes elements are used.

The simulations with concrete lining are performed by activating an elastic beam element on the tunnel surface nodes at the end of the excavation phase. The beam elements are 20 cm thick with Young's modulus of 30 GPa and Poisson's ratio of 0.2 and a unit weight of 2500 kg/m^3.

Table 1. Parameters of the base case corresponding to the eADP calibration of Bulach Opalinus Clay.

Parameter	**Value**	**Unit**	**Description**
$\mathbf{E_p}$	9890	[MPa]	In-plane Young's modulus
$\mathbf{E_t}$	5780	[MPa]	Transverse Young's modulus
ν_p	0.279	-	In-plane Poisson's ratio
ν_{pt}	0.267	-	Transverse Poisson's ratio
$\mathbf{G_t}$	2500	[MPa]	Transverse Shear modulus
β	1.3	-	Frictional coefficient
δ	0.55	-	Plastic hardening onset factor
γ	10.0	[MPa]	Intercept of the yield surface for p=0 MPa
β_θ	0.79	-	Deviatoric section parameter
χ_h	0.002	-	Hardening peak
ψ_d	0.00049	-	Dilatancy evolution
β_d	0.8	-	Residual strength factor
ψ_h	0.98	-	Damage evolution
A	0.4	-	First strength anisotropy constant
B	1.1	-	Second strength anisotropy constant
Ψ	0.304	-	Dilatancy
$\mathbf{A_h}$	1.72	-	Hardening anisotropy constant

The mesh dependency of the Finite Element solution due to the strain-softening response of the constitutive model has been attenuated by using the Abaqus viscous stabilisation of coupled HM procedures (Smith, 2009). A constant damping approach with a damping factor equal to 5e-6 has been adopted. The effect of viscous stabilisation as a mesh dependency mitigation approach has been thoroughly investigated via specific parametric analyses. The results with the adopted damping factor show a negligible mesh dependency in terms of tunnel convergences (Madaschi et al., 2023).

The calibration of advanced constitutive models is challenging due to the complexity of the described material response and the high number of constitutive parameters. Madaschi et al. (2023) performed a detailed calibration of the eADP model on a large experimental dataset made of 13 triaxial undrained tests performed on Bulach Opalinus Clay. The results of the parameter calibration are shown in Table 1.

3 RESULTS OF THE PARAMETRIC GRC CALCULATIONS

The analysis of short- and long-term GRCs provides an effective overview of the ground response to tunnel excavation. In this work, the sensitivity of the GRCs to the fundamental constitutive assumptions of the eADP model is investigated to highlight the critical aspects of the model. In the following, the reference base case corresponds to the calibrated values for Bulach OPA (Table 1). Five further cases are considered:

i. Fully isotropic elastoplastic response for S-strength (loading perpendicular to the bedding planes);
ii. Elastic anisotropy with isotropic strength response (S-strength);
iii. Fully isotropic perfectly plastic (S-strength);
iv. Perfectly plastic anisotropic response with peak strength properties;
v. Perfectly plastic anisotropic response with residual strength properties.

The modified model parameters with respect to the base case calibration for the five additional cases are shown in Table 2.

The material behaviour in triaxial drained conditions with a confining pressure of 13.5 MPa for the six parameter sets is shown in Figure 2 for the loading directions perpendicular and parallel to the bedding plane. As expected, the first two cases show an isotropic strength response, while the two perfectly plastic limit cases bound the base one.

Table 2. Modified parameters with respect to the base calibration for the five cases defined in the comparative study

Parameter	**Base case**	**Isotropic**	**Stiffness anisotropy**	**Perfecly Plastic Isotropic**	**Anis. Perfecly plastic peak**	**Anis. Perfecly plastic residual**
E_p [Mpa]	9890	9890	9890	9890	9890	9890
Et [Mpa]	5780	9890	5780	9890	5780	5780
ν_p	0.279	0.279	0.279	0.279	0.279	0.279
ν_{pt}	0.267	0.279	0.267	0.279	0.267	0.267
Gt [Mpa]	2500	3866.3	2500	3866.3	2500	2500
β	1.3	1.05	1.05	1.05	1.3	1.05
δ	0.55	0.55	0.55	1	1	1
γ [Mpa]	10.0	8.0	8.0	8.0	10.0	8.0
βd	0.8	0.8	0.8	1.	1	1
A	0.4	0	0	0	0.4	0.4
B	1.1	0	0	0	1.1	1.1

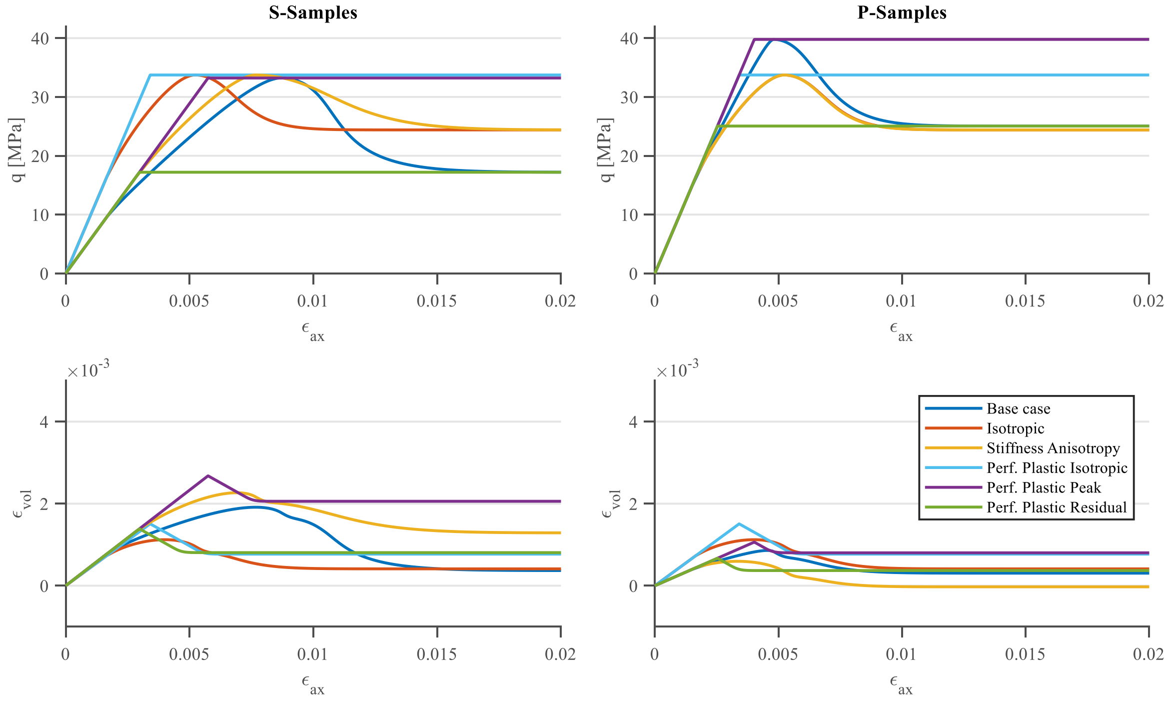

Figure 2. Drained triaxial tests simulations of the five parameter sets used for the GRC simulations.S-Samples: axial loading perpendicular to the bedding planes; P-samples: axial loading parallel to the bedding planes.

Before moving to the GRC, it is worth analysing the tunnel boundary's deformed shape in case of an unsupported excavation. Figure 3 compares the short- and long-term deformed shape between the base case and the two cases that neglect strength anisotropy. It shows a significant increase in convergences due to the consolidation (difference between the short- and the long-term phases) for the base case. Moreover, the base case results show that the most pronounced displacement is observed at the tunnel sidewall with another significant peak at about 55° from the horizontal direction. In addition, it is worth noting that the increment of displacement in the long term for the base case is much higher in correspondence with the tunnel side than at the crown.

a) Short Term

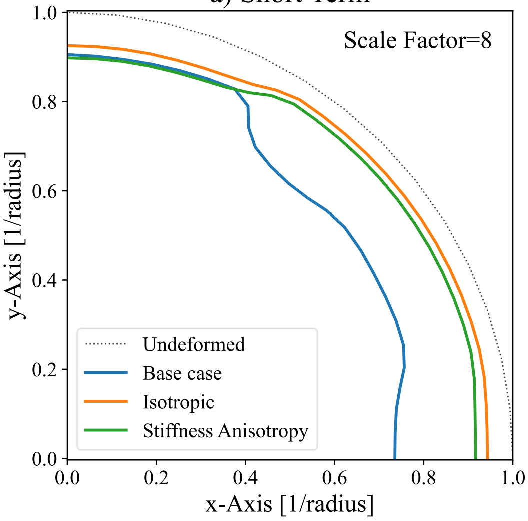

b) Long Term

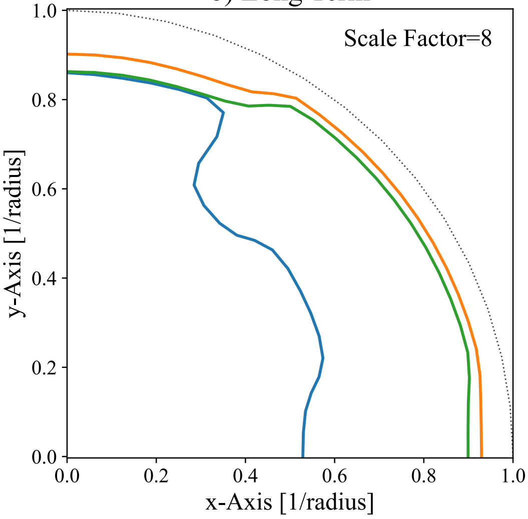

Figure 3. Tunnel surface deformed shape for a non-supported excavation. Impact of the strength anisotropy: a) Short term; b) Long term.

Comparing the simulations performed by deactivating the strength anisotropy ("Isotropic" and "Stiffness anisotropy") highlights the significant effect of this model feature on the ground response. Despite the anisotropy of the elastic material parameters, the effect of the stiffness anisotropy on the deformations of the tunnel contour is small. It should be noted that for the isotropic parameter set, the model response is not fully isotropic (higher displacements at the crown) due to the limited vertical dimension of the Opalinus Clay layer and the proximity to the imposed pore pressure boundary at the crown.

Figure 4 shows the deformed shape comparison between the base case (that includes hardening and softening), the perfectly plastic isotropic, and the two limit cases of an anisotropic linear elastic perfectly plastic model with two parameter sets for the peak and residual strength. As expected, the base case lies between the two limit cases. The base case is closer to the perfectly plastic peak case in correspondence with the tunnel crown and tends to approach the residual strength case moving towards the tunnel side. This observation is consistent with the expected impact of the highly nonlinear material response in the case of a strain-softening response. The plastic isotropic case leads to the smallest deformations and thus shows that the effect of the anisotropic strength is more significant than the softening behaviour.

a) Short Term

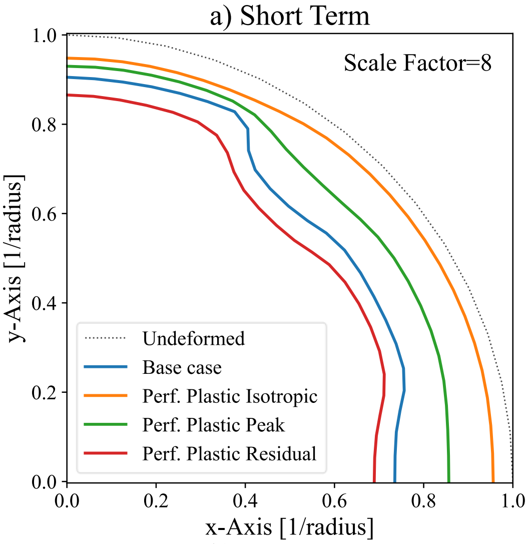

b) Long Term

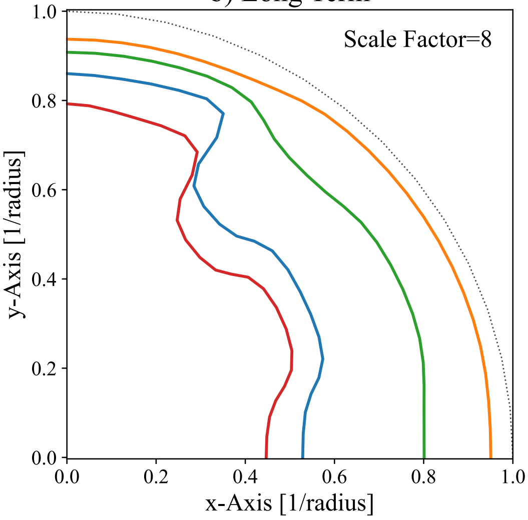

Figure 4. Tunnel surface deformed shape for a non-supported excavation. Impact of model hardening and softening.

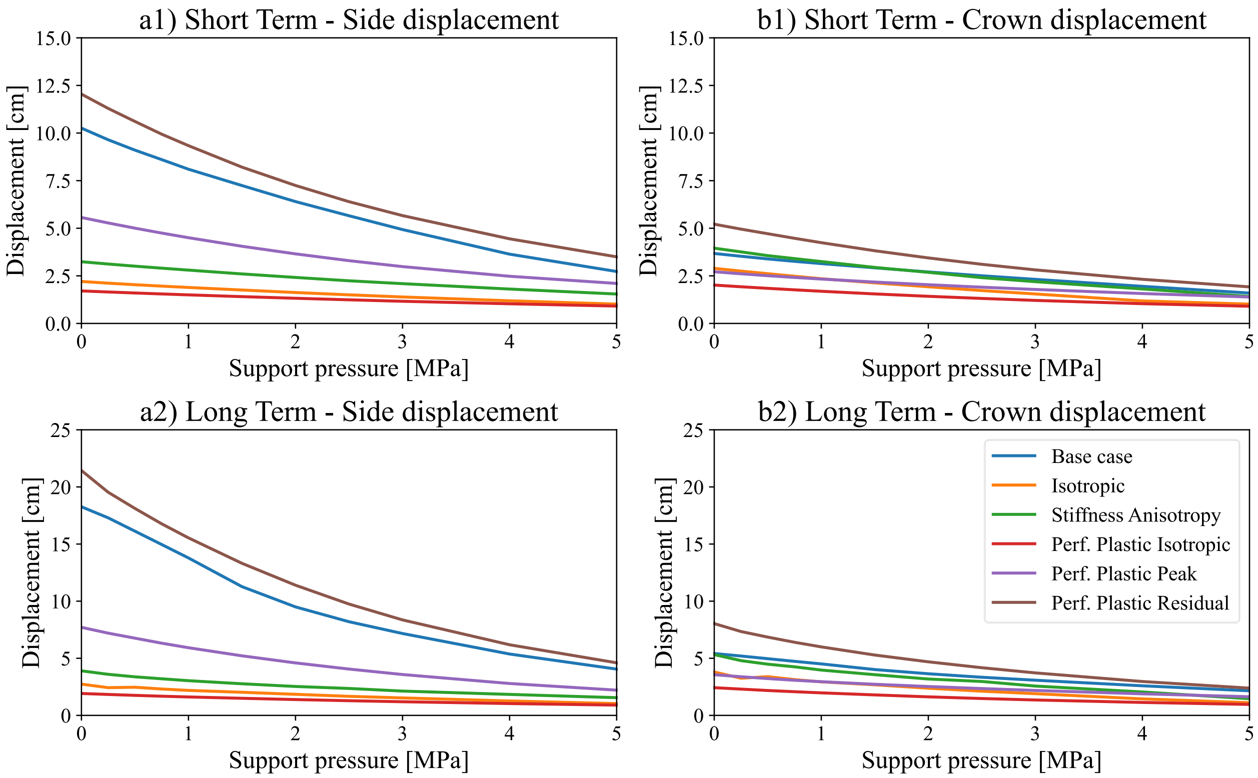

Figure 5. Ground Response Curves for the analysed problem: a) Side displacement; b) Crown displacement.

The GRCs obtained with the six parameter sets are shown in Figure 5. Due to the strong anisotropic response, sidewall and crown GRCs are shown for both short- and long-term.

As already observed in the deformation of the tunnel surface, the strength anisotropy induces a significant asymmetry in the computed displacements between the crown and the side wall. At the crown, the base case GRC is practically coincident with the one computed without strength anisotropy (Figure 5b). On the contrary, the displacements at the tunnel side are significantly higher and tend to be closer to the anisotropic perfectly plastic residual state.

As expected, the impact of strength anisotropy on the GRC is maximum for low support pressures and tends to reduce with increasing tunnel support pressure.

Based on these results, it is possible to highlight that, at the side wall, the perfectly plastic approach with residual strength provides results close to the base case. In contrast, at the crown, displacements for the base case are significantly lower than in the perfectly plastic with residual strength approach. In summary, a perfectly plastic approach (with residual properties) overestimates the displacements at the tunnel wall.

The main outcome of the GRC comparative study is that the greatest impact on the model results is due to the strength anisotropy and not the softening.

The last simulation performed in the context of this study includes the activation of the lining at the end of the excavation phase performed whithout support pressure. This enables evaluating the displacement reduction due to the concrete support and the internal actions developing in the structural elements due to the consolidation process.

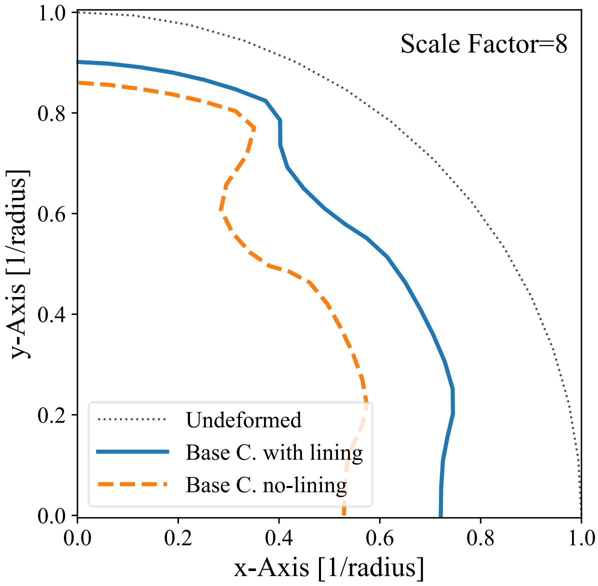

Figure 6. Comparison of the tunnel surface displacements with and without the lining for the base case at the end of the long-term phase.

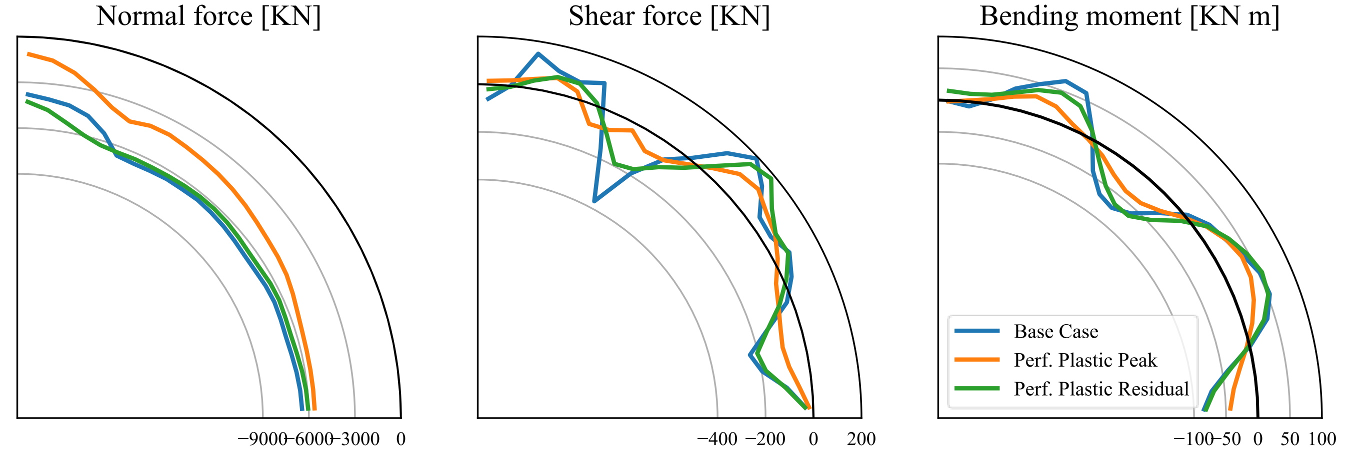

Figure 7. Comparison of the lining internal actions at the end of the simulation (steady state) for the base case and the limit perfectly plastic cases.

Figure 6 compares the base case analyses with and without the concrete lining. As expected, the lining effect is sizeable, with a significant reduction of the convergence in the order of 40 % at the tunnel side. The overall shape of the deformed tunnel is consistent with that without the lining.

The comparison of the internal actions at the end of the simulation for the base case and the two considered perfectly plastic cases (peak and residual strength) is shown in Figure 7. The base case is practically identical to the residual perfectly plastic case. Only locally, the base case provides slightly higher action forces. The peak perfectly plastic case provides, as expected, lower action forces than the base case.

4 CONCLUSIONS

This paper presents a comparative numerical study on tunnel excavation simulations in the context of nuclear waste repositories in Opalinus Clay.

The advanced constitutive model e-ADP is used to describe the material response. This model includes the marked anisotropic behaviour of Opalinus Clay as well as the strong nonlinear stress-strain response (characterised by pre-peak hardening and quasi-brittle softening). The model has been used to compute the Ground Response Curves with a coupled hydro-mechanical plane strain approach that studies the undrained and the long-term ground response. Different parameter sets have been used to emphasise the impact of each fundamental constitutive assumption on the ground response to tunnelling.

The comparative GRC study shows that strength anisotropy is of great importance for the ground response.

In addition, it is worth highlighting that using a perfectly plastic approach with residual parameters provides results close to the model considering softening. Nevertheless, it leads to an overestimation of the displacement at the tunnel wall. In this context, the adoption of validated advanced constitutive models to support the design of nuclear waste repositories can be a crucial factor in optimising the tunnel support design.

Further analyses have been performed to estimate the internal actions developed in the concrete lining during the consolidation process. The anisotropic material response introduces bending and shear actions in the lining. Nevertheless, the high compressive normal forces dominate the internal actions of the lining.

5 REFERENCES

Boldrini, D., Graziani, A. 2012. Remarks on axisymmetric modelling of deep tunnels in argillaceous formations. II: Fissured argillites, *Tunnelling and Underground Space Technology*, **26,** 80-89.

Crisci, E., Giger, S.B., Laloui, L., Ferrari, A., Ewy, R., Stankovic R., Stenebraten J., Halvorsen K., Soldal M. 2023. Large triaxial testing campaign on Opalinus Clay shale from multiple deep boreholes in northern Switzerland, *In preparation*.

Favero, V., Ferrari A., Laloui L. 2016. On the hydro-mechanical behaviour of remoulded and natural Opalinus Clay shale, Engineering Geology **208**, 128-135.

Gautschi, A. 2017. Safety-relevant hydrogeological properties of the claystone barrier of a Swiss radioactive waste repository: An evaluation using multiple lines of evidence, *Grundwasser* **22,** 221–233.

Madaschi, A., Leuthold, J., Cantieni, L., Giger, S.B., Laloui, L. 2023. An advanced numerical anisotropic elastoplastic model for tunnel excavation in the context of geologic nuclear waste repositories, *In preparation*.

Nguyen, X.P., Monfared, M., Bril, O., Armand, G. 2020, Underground Research Laboratory of Bure--Prediction of tunnel behavior during excavation in the short-and long-term based on FLAC3D simulations, *Applied Numerical Modeling in Geomechanics – 2020* (Eds: Billaux, Hazzard, Nelson & Schöpfer) 12-09.

Nordas, A., Cantieni, L., Natale, M., Anagnostou, G. 2023. Study on TBM jamming hazard in Opalinus clay, *World Tunnel Congress 2023.*

Smith, M. 2009. ABAQUS/Standard User's Manual, Version 6.9, *Dassault Systèmes Simulia Corp*, Providence, USA.